Metabolism Open 26 (2025) 100366

Contents lists available at ScienceDirect

Metabolism Open

journal homepage: www.sciencedirect.com/journal/metabolism-open

Comprehensive profiling of candidate biomarkers and immune infiltration landscape in metabolic dysfunction-associated steatohepatitis

Zhangliu Jin [a,1], Jianyun Cao [b,1], Zhaoxun Liu [c,d], Mei Gao [e,*], Hailan Liu [f,**]

[a] Department of General Surgery, The Second Affiliated Hospital of Anhui Medical University, Hefei, Anhui, 230601, China
[b] Reproductive Medicine Center, Xiangya Hospital, Central South University, Changsha, Hunan, 410005, China
[c] Nursing Department, The Third Xiangya Hospital, Central South University, Changsha, Hunan, 410013, China
[d] Department of Emergency, The Third Xiangya Hospital, Central South University, Changsha, Hunan, 410013, China
[e] Department of Pharmacy, Anhui Chest Hospital, Hefei, Anhui, 230000, China
[f] USDA/ARS Children's Nutrition Research Center, Department of Pediatrics, Baylor College of Medicine, Houston, TX, 77030, USA

ARTICLE INFO

Keywords:
Metabolic dysfunction-associated steatohepatitis
Liver
Prognosis
Immune infiltration
Differentially expressed genes

ABSTRACT

Background: The incidence of metabolic dysfunction-associated steatohepatitis (MASH) is increasing, with an incompletely understood pathophysiology involving multiple factors, particularly innate and adaptive immune responses. Given the limited pharmacological treatments available, identification of novel immune metabolic targets is urgently needed. In this study, we aimed to identify hub immune-related genes and potential biomarkers with diagnostic and predictive value for MASH patients.

Methods: The GSE164760 dataset from the Gene Expression Omnibus was utilized for analysis, and the R package was used to identify differentially expressed genes. Immune-related differentially expressed genes (IR-DEGs) were identified by comparing the overlap of differentially expressed genes with well-known immune-related genes. Furthermore, the biological processes and molecular functions of the IR-DEGs were analyzed. To characterize the hub IR-DEGs, we employed a protein-protein interaction network. The diagnostic and predictive values of these hub IR-DEGs in MASH were confirmed using GSE48452 and GSE63067 datasets. Finally, the significance of the hub IR-DEGs was validated using a mouse model of MASH.

Results: A total of 91 IR-DEGs were identified, with 61 upregulated and 30 downregulated genes. Based on the protein-protein interaction network, FN1, RHOA, FOS, PDGFRα, CCND1, PIK3R1, CSF1, and FGF3 were identified as the hub IR-DEGs. Moreover, we found that these hub genes are closely correlated with immune cells. Notably, the validation across two independent cohorts as well as a murine MASH model confirmed their high diagnostic potential.

Conclusion: The hub IR-DEGs, such as FN1, RHOA, FOS, PDGFRα, CCND1, PIK3R1, CSF1, and FGF3, may enhance the diagnosis and prognosis of MASH by modulating immune homeostasis.

1. Introduction

Metabolic dysfunction-associated steatotic liver disease (MASLD) is a prevalent chronic liver condition that affects approximately 25 % of the global population, and is expected to become the leading cause of liver transplantation by 2030, posing a considerable global health challenge [1–4]. MASLD includes a spectrum of liver disorders linked to fat accumulation, ranging from simple steatosis to metabolic dysfunction-associated steatohepatitis (MASH), which is characterized by fat accumulation, hepatocellular injury, inflammation, and fibrosis that may progress to advanced fibrosis and cirrhosis [5]. MASH is closely associated with factors such as age and obesity, and varies by country and ethnicity [6]. In the United States, the direct medical costs for MASLD are estimated to exceed $100 billion annually, with a significant portion dedicated to MASH and related complications [7]. Beyond liver cirrhosis and hepatocellular carcinoma (HCC), MASH markedly increases the risk of extrahepatic complications, including cardiovascular diseases and certain malignancies [8].

* Corresponding author.
** Corresponding author.
E-mail addresses: gaomeizl@126.com (M. Gao), hailan.liu@bcm.edu (H. Liu).
[1] These authors have contributed equally to the work.

https://doi.org/10.1016/j.metop.2025.100366
Received 26 March 2025; Received in revised form 14 April 2025; Accepted 14 April 2025
Available online 15 April 2025

Significant progress has been made in revealing the intricate mechanisms driving MASH progression, which is influenced by a dynamic interplay of environmental factors and host genetics, encompassing both intrahepatic and extrahepatic events [9]. Dysregulation of innate and adaptive immune responses has emerged as a key contributing factor to MASH progression, with immune cell activation and recruitment in the liver often triggered by local or systemic signals from adipose tissue or the gut [1,10]. These signals, associated with microbial imbalances and bacterial translocation, can initiate inflammatory responses that contribute to cellular injury and death, fueling the progression of MASH [11]. A more comprehensive understanding of the immune mechanisms involved in MASH is critical to improve patient outcomes [12]. However, limited data on the transcriptional profiles of individuals with MASH impedes research on the pathogenesis of the disease and hinders biomarker discovery [13]. Identifying and characterizing these biomarkers may enhance the diagnosis and treatment of patients with MASH. Hence, there is an urgent need to identify biomarkers and develop prognostic tools for personalized monitoring and management of MASH.

In this study, hepatic gene expression profiles of patients with MASH and healthy controls were retrieved from the Gene Expression Omnibus (GEO) database (GSE164760) and analyzed using R software. Differentially expressed genes (DEGs) between patients with MASH and healthy controls were identified. Among these DEGs, immune-related DEGs (IR-DEGs) were selected for further analysis. Functional enrichment analysis of IR-DEGs was performed using Gene Ontology (GO) and Kyoto Encyclopedia of Genes and Genomes (KEGG) databases to explore their biological functions [14]. Additionally, a protein-protein interaction (PPI) network was used to identify hub IR-DEGs [15]. Finally, these hub IR-DEGs had a high diagnostic value, which was appraised in two additional cohorts. A flowchart is shown in Supplementary Fig. S1. This study offers valuable insights into MASH pathogenesis, enhances diagnostic and prognostic capabilities, and identifies potential therapeutic targets in patients with MASH.

2. Material and methods

2.1. Microarrays dataset collection and identification of DEGs

The GSE164760 dataset identified using the GPL13667 platform was downloaded from the GEO database. Microarray data of the GSE164760 dataset (74 MASH tissues and 6 healthy controls) were subjected to log2 transformation and normalized using the R package "limma." The ImFit and eBayes methods were applied to evaluate log2 fold change (log2FC). An adjusted P-value <0.05 and transcripts with $|\log2FC| \geq 0.585$ were used as the cutoff for difference analysis, as previously described [16–18].

2.2. Identification of IR-DEGs

As previously reported, DEGs that overlapped with immune-specific marker genes were defined as IR-DEGs and identified using a Venn graph [19,20]. In total, 2498 immune-related genes were documented in the list, along with 782 immune-related genes and 28 common immune cells identified in previous publications [19,20]. A total of 2839 immune-related genes were compiled by combining the data from these two sources and removing duplicates, which were then cross-referenced with DEGs to identify the IR-DEGs.

2.3. Functional enrichment analysis of IR-DEGs

GO and KEGG were used to annotate and analyze the biological functions of the IR-DEGs. GO analyses encompassed the cellular component (CC), biological process (BP), and molecular function (MF) categories. KEGG analysis was utilized to clarify the remarkable pathways for gene enrichment.

2.4. PPI network analysis of IR-DEGs

The STRING database, a comprehensive resource for protein-protein interactions, provides both experimentally validated and predicted interaction information. The combined score suggested an interplay between the two proteins. Additionally, to further analyze the correlations between these proteins, we employed Cytoscape to confirm the hub IR-DEGs within the PPI network.

2.5. Diagnostic values of IR-DEGs

Microarray datasets that evaluated the diagnostic values of IR-DEGs were obtained from the GEO database, which contained GSE48452 (18 MASH tissues and 14 healthy controls) and GSE63067 (9 MASH tissues and 7 healthy controls). These two datasets comprised of MASH tissues and healthy liver tissues. Receiver operating characteristic (ROC) curves were generated to analyze the diagnostic value of the hub IR-DEGs. The diagnostic and predictive values were assessed using the area under the curve (AUC) obtained from the ROC curve analysis.

2.6. A mouse model of MASH

Male C57BL/6J wild-type mice was purchased from Jackson Laboratory at 7 weeks of age. All animals were provided water and a standard chow diet ad libitum after birth and were then randomly divided into two groups: the control group and the MASH group ($n = 4$ mice per group). The animals were housed under a 12/12-h light-dark cycle at room temperature. To induce MASH, the mice were fed a high-fat choline-deficient (HFCD) diet (Research Diets Inc., New Brunswick, NJ, USA) for 12 weeks [21]. The animal study was approved by the Institutional Animal Care and Use Committee in Central South University.

2.7. Quantitative real-time PCR

Mouse tissue samples were snap-frozen in liquid nitrogen and stored at −80 °C for subsequent analysis. Total RNA was extracted from liver tissues using TRIzol Reagent (Invitrogen, USA). Subsequently, 1 μg of RNA was reverse-transcribed into cDNA using a synthesis kit (Thermo Fisher Scientific, USA) [14]. Quantitative real-time PCR was performed using SYBR Green mix (Roche, Switzerland) and quantified using ViiA7 System (Life Technologies, USA). The primer sequences for the target genes are listed in Supplementary Table 1.

2.8. Statistical analysis

All data analyses were performed using R software (version 4.1.0; Vienna, Austria) and Prism9 (Graphpad, San Diego, CA, USA). Statistical analysis of the data was performed using Student's t-test to compare continuous variables between the two groups. P values < 0.05 considered statistically significant. Data are presented as mean ± standard error of the mean (SEM). The relationship between gene expression and immune cells was analyzed using Pearson's correlation coefficient.

3. Results

3.1. The landscape of DEGs

To investigate the differential gene expression in MASH patients, liver gene expression profiles from MASH patients and healthy controls were analyzed using the GEO database (GSE164760 dataset). The correlations between the samples in this dataset were consistent according to the correlation analysis (Supplementary Fig. S2A). Principal component analysis further demonstrated clear differences in gene expression between the MASH and healthy control groups (Supplementary Fig. S2B). DEGs were identified using a $|\log2\ FC|$ threshold of ≥ 0.585

and an adjusted *P*-value < 0.05, as exemplified by previous work [16–18]. The top 10 upregulated genes were THBS2, PHLDB2, BTN3A3, GLUL, CHN2, FDFT1, SGK269, BAZ2B, POLI, and RPL14 (Supplementary Fig. S2C), whereas the top 10 downregulated genes were NNMT, SIK1, CRP, GADD45B, NR4A1, JUNB, SERPINA3, SDS, SAA2, and IGFBP1 (Supplementary Fig. S2C). A heatmap further highlighted the distinct DEG between patients with MASH and healthy controls (Supplementary Fig. S2D).

3.2. Verification of IR-DEGs

Although substantial progress has been made in clarifying the role of immune responses in MASH pathogenesis, there are currently no specific immune-targeted therapies for MASH [22–24]. To identify IR-DEGs between patients with MASH and healthy controls, we screened the DEGs, resulting in 91 IR-DEGs (Fig. 1A), with 61 upregulated and 30 downregulated genes (Supplementary Table 2). Among the upregulated genes, the top 10 were CREBZF, GMFB, CYBB, NCK2, ACVR2A, STX16, PPP3CA, FAS, DOCK9, and IKBKB. Similarly, the top 10 downregulated genes were EWSR1, C8G, GALR3, VNN3, HSPA1A, FOS, CRP, NR4A1, SERPINA3, and SAA2 (Fig. 1B; Supplementary Table 3). Based on the fold-change in IR-DEGs, a heatmap was drawn, showing the top 30 upregulated genes and the top 10 downregulated genes (Fig. 1C).

3.3. GO and KEGG enrichment analysis

To further investigate the potential functions of the identified IR-DEGs, we used the "ClusterProfiler" package for KEGG pathway enrichment and GO functional analysis [25]. The enrichGO function of clusterProfiler was used to categorize IR-DEGs into cellular components, biological processes, and molecular function categories. GO analysis indicated that IR-DEGs enrichment was primarily associated with myeloid cell differentiation (BP; Fig. 2A), cell-substrate junction (CC; Fig. 2B), and signaling receptor activator activity (MF; Fig. 2C). Additionally, the top 5 processes with the smallest *P*-values in each category were visualized using the cNetplot function, revealing that genes such as FOS, CSF1, CCND1, RHOA, FGF3, and PIK3R1 were enriched across multiple terms within BP (Supplementary Fig. S3A), CC (Supplementary Fig. S3B), and MF (Supplementary Fig. S3C). KEGG pathway analysis further demonstrated that upregulated genes were primarily involved in pathways such as Th17 cell differentiation, Th1 and Th2 cell differentiation, human cytomegalovirus infection, and the PI3K/AKT signaling pathway (Supplementary Fig. S4A). Conversely, downregulated genes were enriched in pathways, including the MAPK signaling pathway, COVID-19, Measles, and B cell receptor signaling pathways (Supplementary Fig. S4B). Our results indicate that MASH pathogenesis is not merely a secondary manifestation of chronic liver injury, but rather originates from specific signaling pathways, particularly through immune regulatory mechanisms.

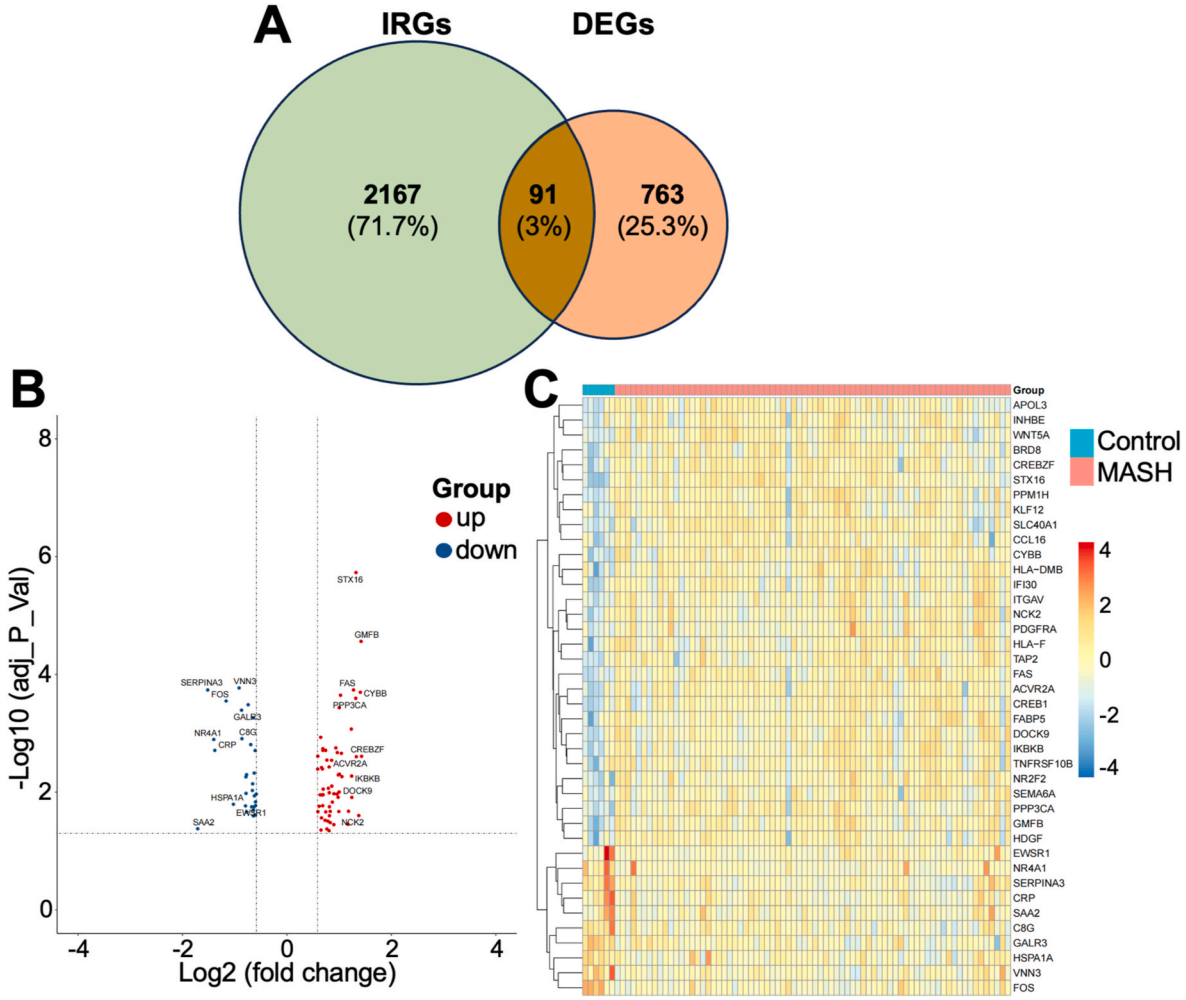

Fig. 1. Verification of IR-DEGs. (A) 91 IR-DEGs were screened out in the GSE164760 dataset. (**B**) A volcano plot of IR-DEGs in the MASH and healthy control groups in the GSE164760 dataset. (**C**) A heatmap of IR-DEGs in the top 30 up-regulated and top 10 down-regulated IR-DEGs in the GSE164760 dataset.

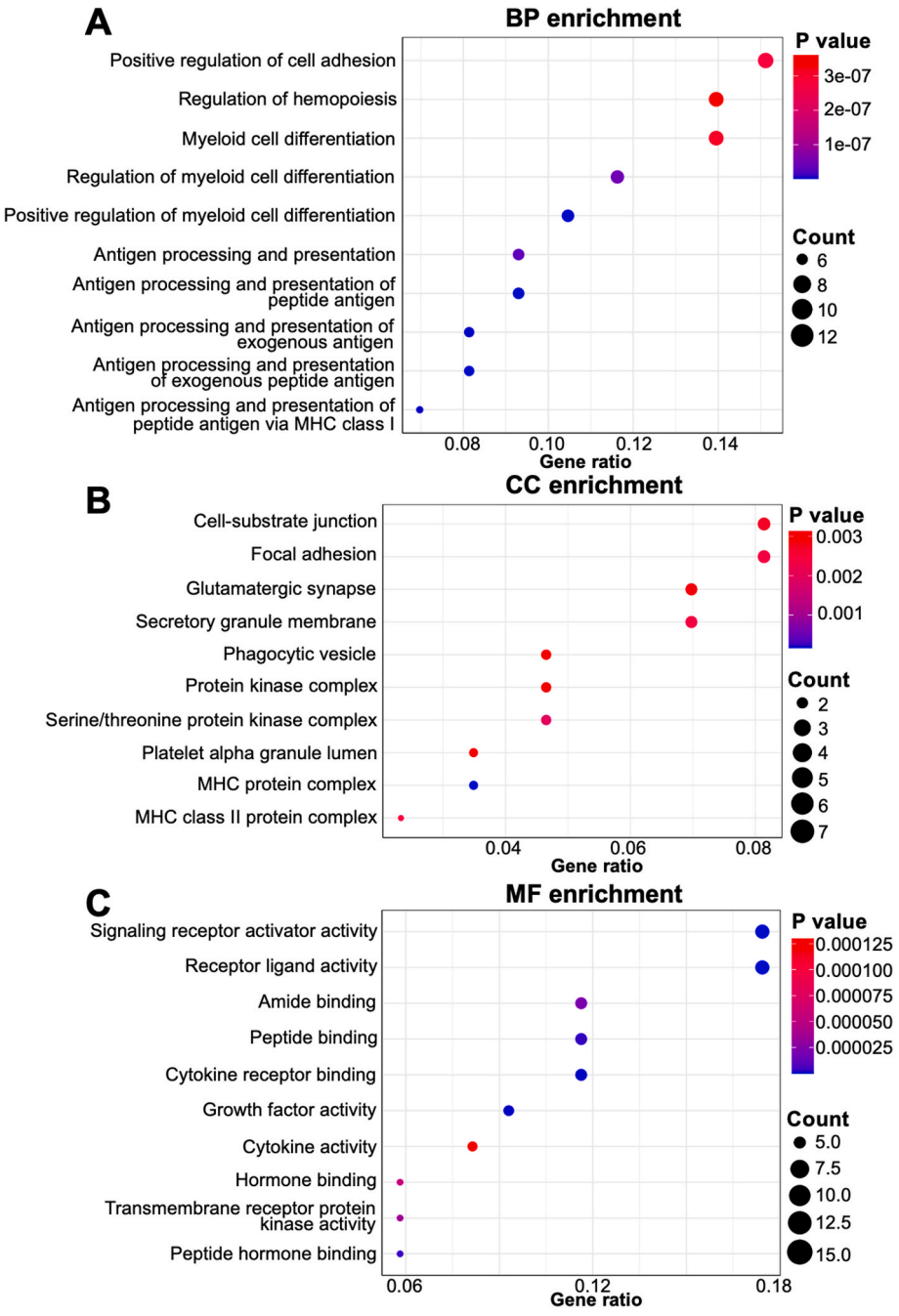

Fig. 2. GO enrichment of IR-DEGs. The dot plots display the top 10 terms enriched by IR-DEGs in BP (**A**), CC (**B**), and MF (**C**) in the GSE164760 dataset.

3.4. Protein-protein interaction network analysis and hub IR-DEGs

A comprehensive PPI network was constructed to identify the key genes associated with MASH [26]. Using the STRING database, we developed a PPI network of 91 IR-DEGs to visualize interactions among their corresponding proteins (Fig. 3A). Two significant sub-clusters emerged, with scores of 6.909 and 9.333, respectively (Fig. 3B and C). Finally, based on the score of degree method, we selected hub genes, such as FN1, RHOA, FOS, PDGFRα, CCND1, PIK3R1, CSF1, and FGF3 (Fig. 3D). Notably, FOS, CCND1, PIK3R1, FN1, and RHOA have previously been linked to MASH [27–31]. In contrast, the roles of PDGFRα, CSF1, and FGF3 in MASH remain unvalidated, highlighting potential novel targets.

3.5. Analysis of immune cells proportion in MASH

The liver is enriched with a diverse array of immune cells, including macrophages, neutrophils, T cells, and natural killer T (NKT) cells [32, 33]. The activation of these cells, along with the subsequent dysregulation of inflammatory cytokine production, exacerbates the hepatocellular injury [34]. Hepatic immune cell populations reshape during MASH and contribute to disease pathogenesis [1]. Knowledge of the changes in immune cell proportions will provide deeper insights into the roles of immune homeostasis in MASH. To this end, we analyzed the differences in immune cell populations in the livers of healthy individuals and those with MASH using the CIBERSORTx algorithm. MASH individuals exhibited higher proportions of activated $CD4^+$ T cells, immature B cells, immature dendritic cells, and NKT cells, and lower proportions of type 17 T helper cells (Fig. 4). Nevertheless, our

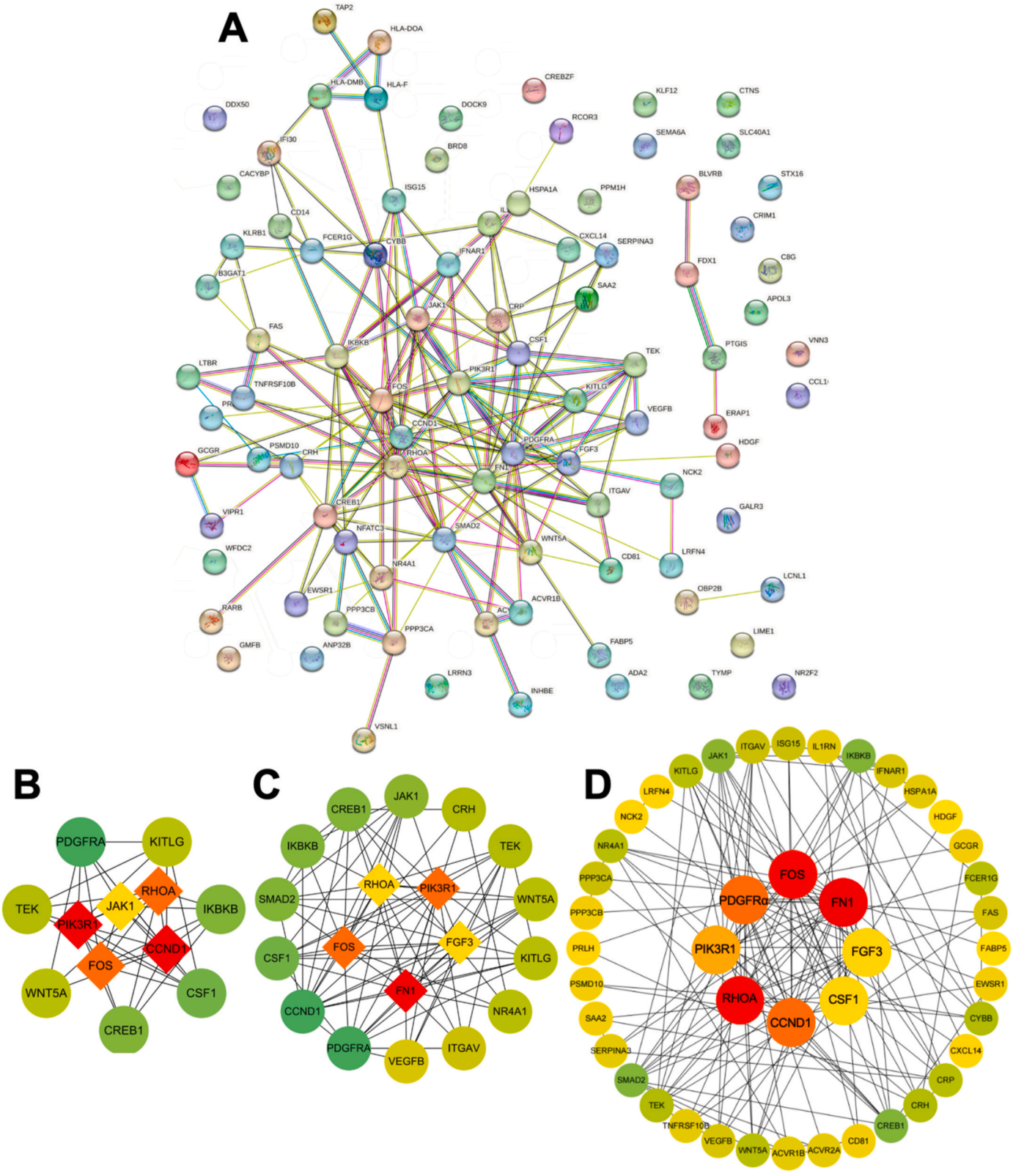

Fig. 3. A PPI network of IR-DEGs. (**A**) A PPI network for 91 IR-DEGs in the GSE164760 dataset. (**B-C**) Sub-clusters of PPI network in the GSE164760 dataset. (**D**) Top 8 hub IR-DEGs of PPI network in the GSE164760 dataset. The circle in the middle represents hub IR-DEGs.

results showed that the proportion of natural killer cells, while increasing, did not change significantly (Fig. 4), which may be due to the small sample size and differences within the groups.

3.6. Correlation of hub IR-DEGs with immune cells in MASH

Given the crucial roles that immune cells play in the progression of MASH [11], we employed bubble diagrams to elucidate the

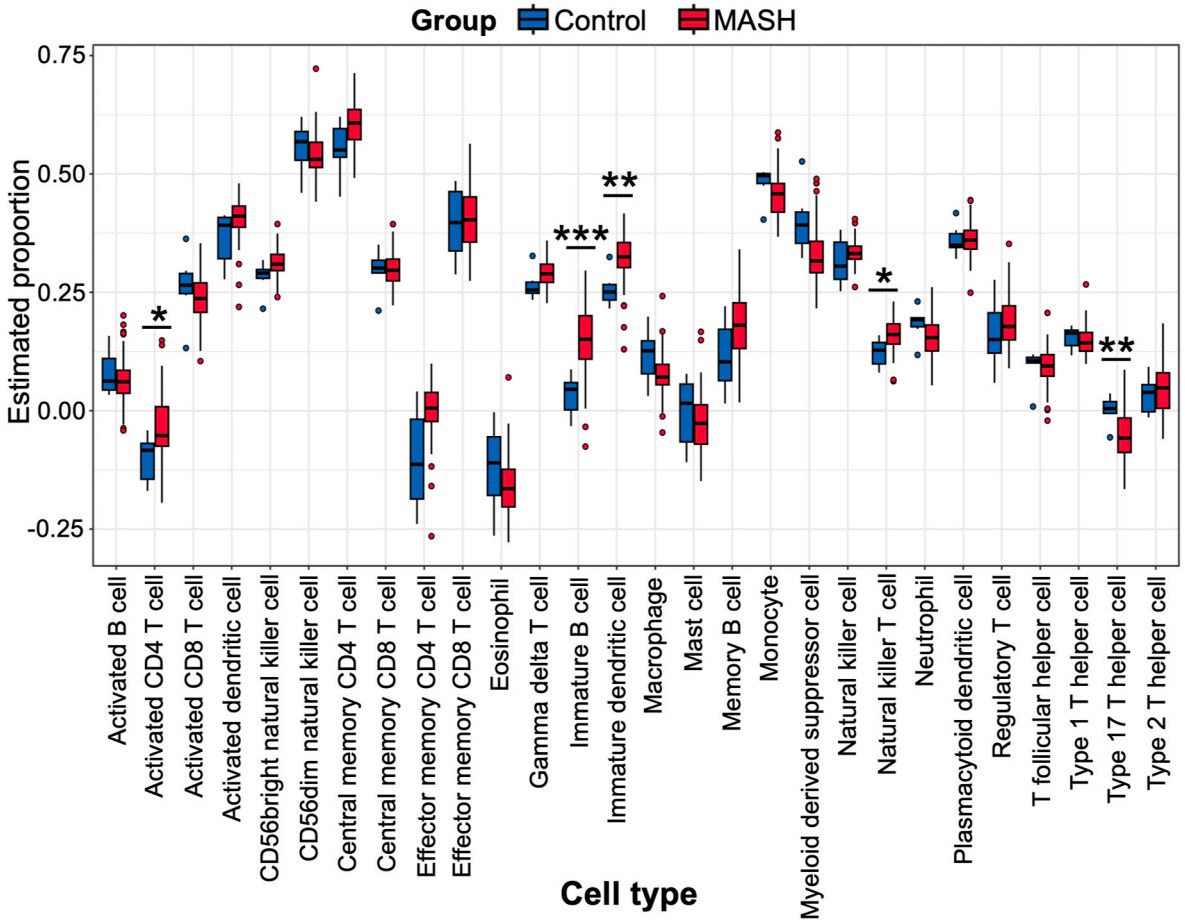

Fig. 4. Immune cell proportions in liver from MASH and healthy individuals in the GSE164760 dataset. *$P < 0.05$; **$P < 0.01$; ***$P < 0.001$.

relationships between hub IR-DEGs and various immune cell populations. PDGFRα was positively associated with central memory $CD4^+$ T cells, activated $CD4^+$ T cells, and effector memory $CD8^+$ T cells (Fig. 5A). CSF1 was positively correlated with CD56bright natural killer cells, immature B cells, and effector memory $CD4^+$ T cells (Fig. 5B). FGF3 positively correlated with macrophages, mast cells, and CD56dim natural killer cells (Fig. 5C). PIK3R1 positively correlated with memory B cells, immature dendritic cells, and CD56bright natural killer cells (Fig. 5D). FOS was positively correlated with macrophages, myeloid-derived suppressor cells, and mast cells (Fig. 5E). CCND1 was positively associated with central memory $CD4^+$ T cells, activated $CD4^+$ T cells, and activated dendritic cells (Fig. 5F). FN1 showed a positive relationship with effector memory $CD4^+$ T cells, memory B cells, and immature dendritic cells (Fig. 5G). Finally, RHOA positively correlated with effector memory $CD4^+$ T cells, activated dendritic cells, and central memory $CD4^+$ T cells (Fig. 5H). These findings indicate that IR-DEGs may play a significant role in immune regulation during MASH progression.

3.7. Diagnostic value of hub IR-DEGs

To evaluate the diagnostic and predictive capabilities of the hub IR-DEGs in MASH, we conducted ROC curve analysis across the two cohorts. In the GSE63067 cohort, the AUC values were 0.825 for CSF1, 0.714 for FGF3, 0.587 for FN1, 0.635 for RHOA, 0.571 for FOS, 0.635 for PDGFRα, 0.571 for CCND1, and 0.603 for PIK3R1, when combined into one variable (Fig. 6A). In the GSE48452 cohort, the AUC values were as follows: 0.571 for CSF1, 0.698 for FGF3, 0.683 for FN1, 0.516 for RHOA, 0.603 for FOS, 0.579 for PDGFRα, 0.663 for CCND1, and 0.524 for PIK3R1, also when these IR-DEGs were combined into a single variable (Fig. 6B). The ROC curve analysis serves as a preliminary screening tool to evaluate the diagnostic potential of candidate hub genes. While some hub genes such as FN1, RHOA, and PIK3R1 showed moderate AUC values, extensive experimental validation is required to confirm these findings. Consequently, to validate our findings further, we investigated the expression of hub IR-DEGs in a mouse model of MASH (Supplementary Fig. S5A and B). The mRNA levels of hub IR-DEGs were consistent with our previous bioinformatic analysis (Fig. 6C). Taken together, these results indicate that PDGFRα, CSF1, FGF3, PIK3R1, FOS, CCND1, FN1, and RHOA exhibit strong diagnostic value in distinguishing patients with MASH from healthy controls.

4. Discussion

In this study, we identified and selected 91 IR-DEGs in the liver of MASH and healthy control subjects from the GSE164760 microarray dataset in GEO. As demonstrated by GO and KEGG analyses, these IR-DEGs were considerably related to immune cell differentiation, B cell receptor signaling pathway, antigen processing, and presentation of peptide antigens. We further clarified that PDGFRα, CSF1, FGF3, FOS, PIK3R1, CCND1, FN1, and RHOA serve as hub IR-DEGs that play pivotal roles in the pathogenesis and progression of MASH. Additionally, our findings indicated that these hub IR-DEGs were closely correlated with immune cells. Finally, we evaluated the diagnostic potential of these hub IR-DEGs, all of which demonstrated strong diagnostic value. This study revealed several hub IR-DEGs that may play central roles in modulating immune infiltration in the liver during MASH progression, thereby providing potential new targets for future MASH diagnosis and therapies in humans.

Enrichment analysis suggested that important pathways are

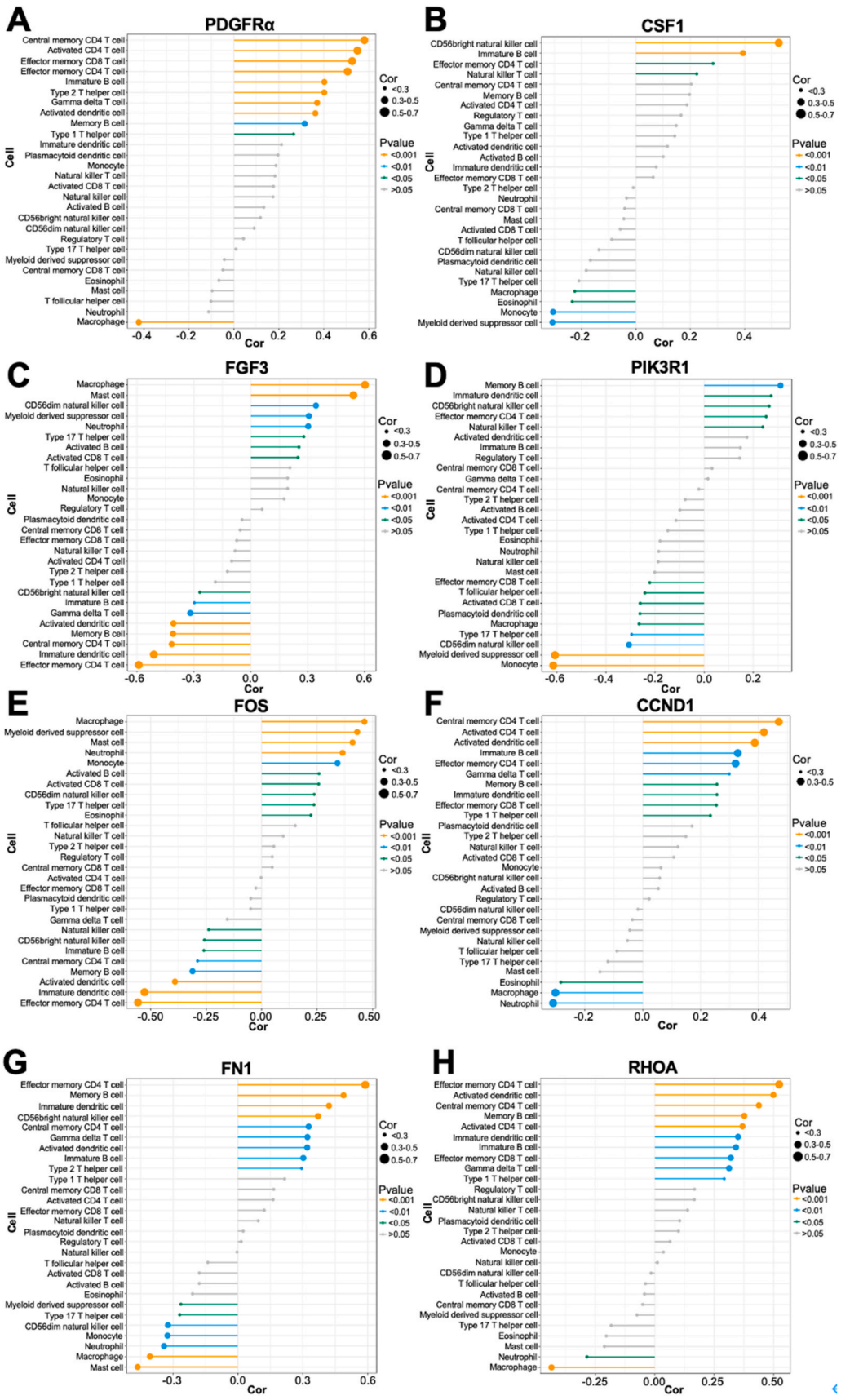

Fig. 5. Relationships between PDGFRα (A), CSF1 (B), FGF3 (C), PIK3R1 (D), FOS (E), CCND1 (F), FN1 (G), and RHOA (H) and immune cells in MASH in the GSE164760 dataset.

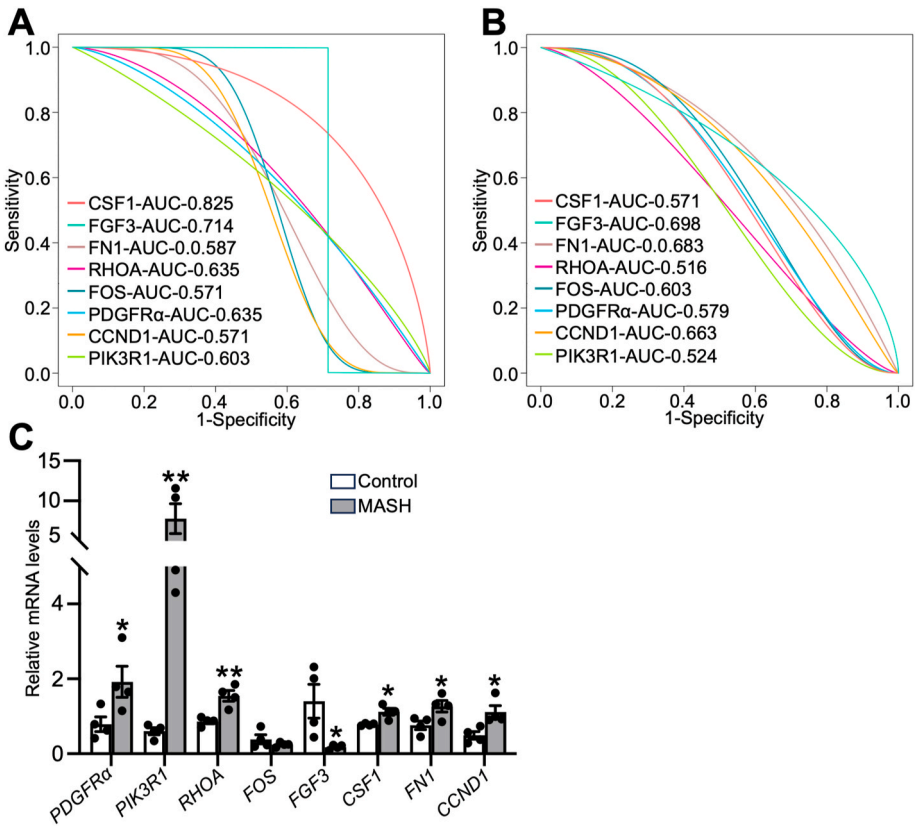

Fig. 6. The Hub IR-DEGs had possessed strong prognostic values in MASH. In the GSE63067 (**A**) and GSE48452 (**B**) datasets, diagnostic values of CSF1, FGF3, FN1, RHOA, FOS, PDGFRα, CCND1, and PIK3R1 in MASH were evaluated. (**C**) The mRNA levels of hub IR-DEGs of liver isolated from a mouse MASH model ($n = 4$/group) . All data are means ± SEM. $^{*}P < 0.05$; $^{**}P < 0.01$.

correlated with immune cell homeostasis, antigen processing and presentation, and the B-cell receptor signaling pathway. Our findings demonstrate a key role for immunity in the pathogenesis of MASH. Our results may also partly explain why MASH is a risk factor for worse COVID-19 clinical outcomes and other infectious diseases, such as human cytomegalovirus infection, human T cells leukemia virus 1 infection, and Epstein-Barr virus infection, as shown by KEGG analysis [35–39]. Given the significant role of immunology in MASH pathogenesis and progression, we dissected several upregulated immune cells, including NKT cells, immature dendritic cells, activated $CD4^+$ T cells, and immature B cells. The accumulation of NKT cells is correlated with exacerbated fibrosis in MASH [40], and LIGHT secreted by these cells has been shown to activates NF-κB signaling, which facilitates steatosis and the transition from MASH to HCC [41]. Moreover, during hepatic injury in MASH, dendritic cells adopt an immunogenic phenotype characterized by an enhanced capacity to present antigens and increased production of proinflammatory cytokines [42]. Despite divergent reports regarding the shift in the total number of hepatic $CD4^+$ T cells in MASLD, the existing literature suggests that the polarization of $CD4^+$ T cells towards Th1 and Th17 subsets, along with increased production of IFNγ and IL-17A, contributes to the progression of MASH [1]. Additionally, the accrual of hepatic B cells has been observed in humans with MASH, which is accompanied by elevated expression of inflammatory mediators, including IL-6 and TNF [43].

While the associations between certain hub IR-DEGs, such as FOS, PIK3R1, CCND1, FN1, RHOA, and MASH, are well established, the roles of PDGFRα, CSF1, and FGF3 in the onset and progression of MASH are less understood and warrant further investigation [27–31]. Although the regulatory roles of these hub genes including FN1, RHOA, FOS, CCND1, and PIK3R1 in MASH pathogenesis have been well-characterized in prior studies [27–31], their potential immunomodulatory functions - particularly in relation to immune cells interaction-remain underexplored. Our findings revealed significant associations between these hub genes and diverse immune cell populations, suggesting their potential involvement in MASH pathogenesis through immune signaling networks. While the direct association between hub genes, such as PDGFRα, CSF1, and FGF3 and MASH pathogenesis remains unreported in existing literature, their established connection with immune-related pathways warrants attention [44–46]. Given that immune signaling dysregulation represents a pivotal mechanistic component in MASH progression, our investigation demonstrates significant correlations between these hub genes and immune cell dynamics (Fig. 5A–C). This suggests their potential involvement in MASH pathogenesis through immunomodulatory mechanisms. Firstly, platelet-derived growth factor receptor alpha (PDGFRα) encodes a receptor tyrosine kinase that plays a crucial role in various physiological processes related to human growth and development [47]. Upon binding to its ligand, PDGF and PDGFRα undergo dimerization and phosphorylation, activating several downstream signaling pathways, including the PI3K/AKT, MAPK/ERK, JAK/STAT, and Notch pathways. Although PDGFRα is pivotal in gastrointestinal stromal tumors, its involvement in MASH progression remains unexplored. As PDGFRα is positively correlated with $CD4^+$ T cells, we propose that upregulation of PDGFRα may contribute to immune cell recruitment in MASH. Furthermore, colony stimulating factor 1 (CSF1), which is produced in a membrane-bound form by fibroblasts and tumor cells, is an essential growth factor required for regulating macrophage proliferation and differentiation [45,48]. In this study, we found that CSF1 was upregulated and positively related to NKT cells in the MASH group. These results indicate that elevated CSF1 levels in MASH may aggravate inflammation and fibrosis. Fibroblast growth factor 3 (FGF3), initially identified in the ventral hypothalamus, is crucial during embryonic development [49]. Although extensive studies have focused on

its conserved role in hindbrain development, the specific role of FGF3 in modulating MASH remains to be clarified based on its dynamic expression patterns. We found that FGF3 was downregulated in MASH and negatively correlated with immature dendritic cells and B cells, suggesting that decreased FGF3 may play a pathogenic role in MASH progression. Collectively, based on our findings from both the diagnostic performance of AUC and mRNA dysregulation in the murine MASH model, we speculate that FGF3 may serve as the most promising therapeutic target for MASH treatment.

This study has several limitations that present opportunities for future research. While some of our findings corroborate those of previous research, the sample size was relatively small, which may affect the generalizability of our results. Furthermore, *in vivo* and *in vitro* experiments are necessary to validate the roles of the identified genes in the pathogenesis of MASH and to assess their potential as therapeutic targets for MASH treatment. Although the HFCD diet-induced murine model is widely recognized for recapitulating key features of MASH [50], it is critical to emphasize that current animal models do not fully recapitulate all aspects of human MASH pathophysiology. Consequently, while validation in this murine model provides valuable mechanistic insights, further clinical studies are necessary before incorporating these genes into diagnostic panels for MASH patients.

5. Conclusions

This study identified PDGFRα, CSF1, FGF3, FOS, PIK3R1, CCND1, FN1, and RHOA as potential auxiliary diagnostic indicators of MASH. Our research provides both theoretical and experimental insights that enhance the understanding of MASH pathogenesis and improve its diagnostic and prognostic capabilities. However, further validation is required through the analysis of additional samples from clinical MASH patients to substantiate these findings.

CRediT authorship contribution statement

Zhangliu Jin: Writing – original draft, Funding acquisition, Conceptualization. **Jianyun Cao:** Formal analysis. **Zhaoxun Liu:** Visualization. **Mei Gao:** Writing – review & editing, Writing – original draft. **Hailan Liu:** Writing – review & editing, Funding acquisition.

Data availability

Publicly available datasets were analyzed in this study. These data can be obtained from the http://www.ncbi.nlm.nih.gov/geo, GSE164760 GSE48452, and GSE63067 datasets.

Funding

This work was supported by grants from the National Natural Science Foundation of China (82400738), Natural Science Foundation of Anhui Province (2408085QH267), and American Heart Association (23POST1030352).

Conflict of interest

The authors declare no conflict of interests.

Acknowledgements

We thank the GEO database for providing free data on MASH.

Appendix A. Supplementary data

Supplementary data to this article can be found online at https://doi.org/10.1016/j.metop.2025.100366.

References

[1] Sawada K, Chung H, Softic S, et al. The bidirectional immune crosstalk in metabolic dysfunction-associated steatotic liver disease. Cell Metab 2023;35(11):1852–71.
[2] Tacke F, Puengel T, Loomba R, et al. An integrated view of anti-inflammatory and antifibrotic targets for the treatment of NASH. J Hepatol 2023;79(2):552–66.
[3] Lonardo A, Mantovani A, Petta S, et al. Metabolic mechanisms for and treatment of NAFLD or NASH occurring after liver transplantation. Nat Rev Endocrinol 2022;18(10):638–50.
[4] Wang X, Zhang L, Dong B. Molecular mechanisms in MASLD/MASH-related HCC. Hepatology 2024;13(10):1097.
[5] Vitale A, Svegliati-Baroni G, Ortolani A, et al. Epidemiological trends and trajectories of MAFLD-associated hepatocellular carcinoma 2002-2033: the ITA.LI.CA database. Gut 2023;72(1):141–52.
[6] Schneider CV, Schneider KM, Raptis A, et al. Prevalence of at-risk MASH, MetALD and alcohol-associated steatotic liver disease in the general population. Aliment Pharmacol Ther 2024;59(10):1271–81.
[7] Tincopa MA, Anstee QM, Loomba R. New and emerging treatments for metabolic dysfunction-associated steatohepatitis. Cell Metab 2024;36(5):912–26.
[8] Wang S, Friedman SL. Found in translation-Fibrosis in metabolic dysfunction-associated steatohepatitis (MASH). Sci Transl Med 2023;15(716):eadi0759.
[9] Allen AM, Younossi ZM, Diehl AM, et al. Envisioning how to advance the MASH field. Nat Rev Gastroenterol Hepatol 2024;21(10):726–38.
[10] Li Z, Wang S, Xu Q, et al. The double roles of T cell-mediated immune response in the progression of MASLD. Biomed Pharmacother 2024;173:116333.
[11] Rabiu L, Zhang P, Afolabi LO, et al. Immunological dynamics in MASH: from landscape analysis to therapeutic intervention. J Gastroenterol 2024;59(12):1053–78.
[12] Cheu JW, Wong CC. The immune microenvironment of steatotic hepatocellular carcinoma: current findings and future prospects. Hepatol Commun 2024;8(9):e0516.
[13] Pericàs JM, Anstee QM, Augustin S, et al. A roadmap for clinical trials in MASH-related compensated cirrhosis. Nat Rev Gastroenterol Hepatol 2024;21(11):809–23.
[14] Jin Z, Dou M, Peng W, et al. Identification of distinct immune infiltration and potential biomarkers in patients with liver ischemia-reperfusion injury. Life Sci 2023;327:121726.
[15] Mohseni Behbahani Y, Saighi P, Corsi F, et al. LEVELNET to visualize, explore, and compare protein-protein interaction networks. Proteomics 2023;23(17):e2200159.
[16] Jensen VS, Fledelius C, Zachodnik C, et al. Insulin treatment improves liver histopathology and decreases expression of inflammatory and fibrogenic genes in a hyperglycemic, dyslipidemic hamster model of NAFLD. J Transl Med 2021;19(1):80.
[17] Bharati J, Kumar S, Mohan NH, et al. Ovarian follicle transcriptome dynamics reveals enrichment of immune system process during transition from small to large follicles in cyclic Indian Ghoongroo pigs. J Reprod Immunol 2023;160:104164.
[18] Zhang Z, Qiao Y, Ji J, et al. The potential role of differentially expressed tRNA-derived fragments in high glucose-induced podocytes. Ren Fail 2024;46(1):2318413.
[19] Bhattacharya S, Andorf S, Gomes L, et al. ImmPort: disseminating data to the public for the future of immunology. Immunol Res 2014;58(2–3):234–9.
[20] Bindea G, Mlecnik B, Tosolini M, et al. Spatiotemporal dynamics of intratumoral immune cells reveal the immune landscape in human cancer. Immunity 2013;39(4):782–95.
[21] Bu L, Zhang Z, Chen J, et al. High-fat diet promotes liver tumorigenesis via palmitoylation and activation of AKT. Gut 2024;73(7):1156–68.
[22] Yashaswini CN, Qin T, Bhattacharya D, et al. Phenotypes and ontogeny of senescent hepatic stellate cells in metabolic dysfunction-associated steatohepatitis. J Hepatol 2024;81(2):207–17.
[23] Wang H, Tsung A, Mishra L, et al. Regulatory T cell: a double-edged sword from metabolic-dysfunction-associated steatohepatitis to hepatocellular carcinoma. EBioMedicine 2024;101:105031.
[24] Pipitone RM, Lupo G, Zito R, et al. The PD-1/PD-L1 Axis in the biology of MASLD. Int J Mol Sci 2024;25(7):3671.
[25] Xu S, Hu E, Cai Y, et al. Using clusterProfiler to characterize multiomics data. Nat Protoc 2024;19(11):3292–320.
[26] Gao H, Sun X, Liu Y, et al. Analysis of hub genes and the mechanism of immune infiltration in stanford type a aortic dissection. Front Cardiovasc Med 2021;8:680065.
[27] Tsay A, Wang JC. The role of PIK3R1 in metabolic function and insulin sensitivity. Int J Mol Sci 2023;24(16):12665.
[28] Oh HY, Shin SK, Heo HS, et al. Time-dependent network analysis reveals molecular targets underlying the development of diet-induced obesity and non-alcoholic steatohepatitis. Genes Nutr 2013;8(3):301–16.
[29] Cai C, Chen DZ, Tu HX, et al. MicroRNA-29c acting on FOS plays a significant role in nonalcoholic steatohepatitis through the interleukin-17 signaling pathway. Front Physiol 2021;12:597449.
[30] Moreto F, Ferron AJT, Francisqueti-Ferron FV, et al. Differentially expressed proteins obtained by label-free quantitative proteomic analysis reveal affected biological processes and functions in Western diet-induced steatohepatitis. J Biochem Mol Toxicol 2021;35(6):1–11.
[31] Ye Q, Liu Y, Zhang G, et al. Deficiency of gluconeogenic enzyme PCK1 promotes metabolic-associated fatty liver disease through PI3K/AKT/PDGF axis activation in male mice. Nat Commun 2023;14(1):1402.
[32] Guilliams M, Scott CL. Liver macrophages in health and disease. Immunity 2022;55(9):1515–29.

[33] Cheng ML, Nakib D, Perciani CT, et al. The immune niche of the liver. Clin Sci (Lond) 2021;135(20):2445–66.
[34] Hu C, Wu Z, Li L. Mesenchymal stromal cells promote liver regeneration through regulation of immune cells. Int J Biol Sci 2020;16(5):893–903.
[35] Hoffmann C, Gerber PA, Cavelti-Weder C, et al. Liver, NAFLD and COVID-19. Horm Metab Res 2022;54(8):522–31.
[36] Moore JB. COVID-19, childhood obesity, and NAFLD: colliding pandemics. Lancet. Gastroenterol. Hepatol. 2022;7(6):499–501.
[37] Khiatah B, Nasrollah L, Covington S, et al. Nonalcoholic fatty liver disease as a risk factor for cytomegalovirus hepatitis in an immunocompetent patient: a case report. World J Clin Cases 2021;9(6):1455–60.
[38] Nayan SI, Rahman MH, Hasan MM, et al. Network based approach to identify interactions between Type 2 diabetes and cancer comorbidities. Life Sci 2023;335:122244.
[39] Wyss J, Raselli T, Wyss A, et al. Development of non-alcoholic steatohepatitis is associated with gut microbiota but not with oxysterol enzymes CH25H, EBI2, or CYP7B1 in mice. BMC Microbiol 2024;24(1):69.
[40] Syn WK, Oo YH, Pereira TA, et al. Accumulation of natural killer T cells in progressive nonalcoholic fatty liver disease. Hepatology 2010;51(6):1998–2007.
[41] Wolf MJ, Adili A, Piotrowitz K, et al. Metabolic activation of intrahepatic CD8+ T cells and NKT cells causes nonalcoholic steatohepatitis and liver cancer via cross-talk with hepatocytes. Cancer Cell 2014;26(4):549–64.
[42] Heymann F, Tacke F. Immunology in the liver–from homeostasis to disease. Nat Rev Gastroenterol Hepatol 2016;13(2):88–110.
[43] Kremer M, Hines IN, Milton RJ, et al. Favored T helper 1 response in a mouse model of hepatosteatosis is associated with enhanced T cell-mediated hepatitis. Hepatology 2006;44(1):216–27.
[44] Akiyama T, Yasuda T, Uchihara T, et al. Stromal reprogramming through dual pdgfrα/β blockade boosts the efficacy of anti-PD-1 immunotherapy in fibrotic tumors. Cancer Res 2023;83(5):753–70.
[45] Stanley TL, Fourman LT, Wong LP, et al. Growth hormone releasing hormone reduces circulating markers of immune activation in parallel with effects on hepatic immune pathways in individuals with HIV-infection and nonalcoholic fatty liver disease. Clin Infect Dis 2021;73(4):621–30.
[46] Sehgal A, Irvine KM, Hume DA. Functions of macrophage colony-stimulating factor (CSF1) in development, homeostasis, and tissue repair. Semin Immunol 2021;54:101509.
[47] Cicala CM, Olivares-Rivas I, Aguirre-Carrillo JA, et al. KIT/PDGFRA inhibitors for the treatment of gastrointestinal stromal tumors: getting to the gist of the problem. Expert Opin Investig Drugs 2024;33(3):159–70.
[48] Tacke F, Wynn TA. Biomarker and therapeutic potential of CSF1 in acute liver failure. Gastroenterology 2015;149(7):1675–8.
[49] Huang H, Chen Q, Xu Z, et al. FGF3 directs the pathfinding of prethalamic GABAergic axons. Int J Mol Sci 2023;24(19):14998.
[50] Lan T, Jiang S, Zhang J, et al. Breviscapine alleviates NASH by inhibiting TGF-β-activated kinase 1-dependent signaling. Hepatology 2022;76(1):155–71.